

STUDY OF BLAST WAVE PROBLEM IN A NON-IDEAL DUSTY GAS

Abstract

We develop a generalized analytical method for obtaining an exact solution to adiabatic blast wave problems for one dimensional non-ideal gas flow with dust particles. The total energy carried by a shock wave in a non-ideal dusty gas medium is determined using an assumption that density in front of the shock wave depends on a power of the distance from the source of explosion.

Keywords: Blast Wave; Non-ideal Gas; Dusty Gas; Analytical Solution; Total Energy.

Authors

S. D. Ram

Department of Mathematics
Shivaji College
University of Delhi
Delhi, India.

J. P. Chaudhary

Department of Mathematics
T. D. P. G. College
Jaunpur, India.

L. P. Singh

Department of Mathematical Sciences
Indian Institute of Technology
Banaras Hindu University
Varanasi, India.

I. INTRODUCTION

In dusty gases small solid particles are mixed with gas. The study of blast wave problems for non-ideal dusty gases has several applications in industrial processes as well as geophysical flows. Many natural phenomena are characterized by very small solid particle fractions relative to gas particles, such as volcanic eruptions and rocket exhaust. When a mixture of dust and gas is moving at very high speeds, the mixture behaves like a pseudo-fluid.

If a large amount of energy is released from the core, then an abrupt disturbance in the medium is accompanied by a compressive wave called a blast wave. A system of quasilinear hyperbolic PDEs may be formulated mathematically to model such phenomena. To find the exact solution of the system of equations governing the blast wave problem is almost impossible.

In past many attempts have been made to find the analytical/approximate analytical solution of governing system of the blast wave problem using physically relevant assumptions. Taylor [1, 2] estimated the relationship between the energy input of an extremely powerful explosion and the growth of the resulting fireball and a detailed analysis of Taylor work is presented by Sedov [3]. Rogers [4] has been made a complete investigation for the adiabatic gas of spherically symmetrical flows when undisturbed density is varies as a power of the radius of strong shock wave. Sachdev et al. [5] solved the compressible flow equations in spherically symmetric coordinate system for ordinary gas. Murata [6] introduced a novel approach to address the challenge of solving the blast wave problem analytically. Their innovative method is based on an assumption on the density ahead of shock. This pioneering work marked a significant advancement in the field. Building upon the Murata's foundational research, Singh et al. [7] extended the results. Specifically, they adapted Murata's ideas to the context of non-ideal gases, broadening the scope of the original work.

The foundational effort in the field of investigating shock wave in dusty gas was initiated by Pai [8], Miura and Glass [9], and Chandha and Jena [10]. Diaz and Rigby [11] have made significant contributions to the field of blast wave kinetics. His work has been instrumental in advancing our understanding of the fundamental principles governing the behavior of blast wave. Their research has encompassed various aspects of blast wave kinetics, including the study of shock wave propagation, the dynamics of high energy explosions, and the characterization of blast wave profiles. Bira and Shekhar [12] have obtained the exact solution to the problem of propagation of shock wave in isentropic magnetogasdynamics using symmetry group analysis. Sharma and Shyam [13] conducted a comprehensive investigation into the intricate characteristics of weak shock waves within a radiating gas medium. Their research was indicated to the systematic examination of both the growth and decay patterns exhibited by these shock waves. Sharma and Arora [14] investigated the behavior of one dimensional spherical strong shock wave in non-ideal radiative magnetogasdynamics regime by using the method of Lie group analysis

As blast wave theory is used for a wide range of applications, a continuous improvement in the field is desirable. Since blast waves contain small dust particles and gas, therefore studying blast wave problems for dusty non-ideal gas is more realistic than studying ordinary gas dynamics. In this Chapter, we endeavor to find a closed-form solution for the

equations governing blast wave motion in non-ideal dusty gases. We make an assumption that the density ahead of the shock front varies with distance from the source. Additionally, in the last section, we introduce a formula for calculating the total energy carried by blast waves in non-ideal dusty gas mediums that deviate from ideal conditions

II. FUNDAMENTAL EQUATIONS

Here it is assumed that the dust particles are small solid sphere of identical mass m_s , radius r_s and specific heat c_s . Consider an element of non-ideal dusty gas with mass $M = M_g + M_s$ and volume $V = V_g + V_s$, where the subscripts g and s stand for non-ideal gas and dust particles respectively unless it is specified. The volume of the solid particles in the mixture may be given as

$V_s = n_s V \tau_s$, where $\tau_s = \frac{4}{3} \pi r_s^3$ is the volume of solid particles in non-ideal dusty gas and n_s is

the number of solid dust particles per unit volume of non-ideal dusty gas in an element. The mass of solid dust particles in the non-ideal dusty gas may be given as

$$M_s = m_s n_s V.$$

Also, the species density of solid particles is $\rho_s = \frac{M_s}{V_s} = \frac{m_s}{\tau_s}$. Also, solid particles are assumed to be spherical with same mass and same radius.

An adiabatic non-ideal dusty gas flow can be described by the governing equations given by (Miura and Glass [9], and Chandha and Jena [10])

$$\frac{\partial \rho}{\partial t} + \mathcal{G} \frac{\partial \rho}{\partial x} + \rho \left(\frac{\partial \mathcal{G}}{\partial x} + \frac{m}{x} \mathcal{G} \right) = 0 \quad (1)$$

$$\frac{\partial \mathcal{G}}{\partial t} + \mathcal{G} \frac{\partial \mathcal{G}}{\partial x} + \frac{1}{\rho} \frac{\partial p}{\partial x} = 0 \quad (2)$$

$$\frac{\partial p}{\partial t} + u \frac{\partial p}{\partial x} + c^2 \rho \left(\frac{\partial \mathcal{G}}{\partial x} + \frac{m}{x} \mathcal{G} \right) = 0 \quad (3)$$

where $\rho > 0$ represents density, \mathcal{G} represents velocity and p represents pressure of the non-ideal dusty gas whereas $t > 0$ and $x \in \mathbb{R}$ are stand for time and space coordinate axes. In non-ideal dusty gas, we can define the velocity of sound as $c = \left(\left((\Gamma - \alpha_2 \rho^2) p \right) / \left((1 - \alpha_1 \rho + \alpha_2 \rho^2) \rho \right) \right)^{1/2}$ denotes the speed of sound in the non-ideal dusty gas with $\alpha_1 = \theta + \bar{b}$, $\alpha_2 = \theta \bar{b}$, $\bar{b} = b(1 - k_p)$, where b is denoting the excluded volume of Van der Waals. Here, mass fraction of solid particles in the mixture is denoted by k_p and defined as $k_p = M_s / M$, where M_s is the mass of solid particles and M is the total mass of the considered gas with dust particles. The parameter m takes on different values to represent

district flow configurations: $m=0$ corresponds to planar flow, $m=1$ indicates cylindrical symmetrical flow and $m=2$ signifies spherically symmetrical flow.

A non-ideal dusty gas at constant pressure has a specific heat equal to $c_{tp} = k_p c_p + (1-k_p) c_s$, where c_p indicates the specific heats of gas at constant pressure and c_s stands for the specific heats of solid particles.

If c_{tv} stands for the specific heats of the mixture, the ratio of specific heats is denoted Γ by and defined as

$$\Gamma = \frac{c_{tp}}{c_{tv}} = \gamma(1 + \delta\beta)(1 + \delta\beta)^{-1},$$

where $\delta = k_p / (1-k_p)$, $\beta = c_s / c_p$, $\gamma = c_p / c_v$, c_v specific heat of gas at constant volume. Equation of state for adiabatic non-ideal dusty gas flow is given by [14],

$$p = \frac{(1-k_p)}{(1-Z)(1-\bar{b}\rho)} \rho RT, \text{ in which } Z \text{ is the volume fraction of solid particle in the mixture.}$$

The volume fraction Z and mass fraction k_p are interrelated through the equation

$$Z = \frac{k_p}{(1-k_p)\Omega + k_p}, \text{ where } \Omega = \rho_s / \rho, \rho \text{ signifies the density of the mixture in undisturbed}$$

region. Since the ratio of the density of solid particles in undisturbed region to the total density of the mixture is taken as constant. Therefore, in undisturbed region Ω is constant.

III. BOUNDARY CONDITIONS

The expression for the propagation velocity of the shock front in terms of R (the position of the shock front from the center of explosion) and t (time) is given as

$$s = \frac{dR}{dt} \tag{4}$$

If ahead of shock front the undisturbed volume fraction of solid particles and density of the mixture are Z_0, ρ_0 and pressure, density, velocity just behind the shock are p, ρ, g . Then we have the following Rankine-Huguenot condition across the shock front (Sharma and Arora [14]).

$$\rho = \frac{\Gamma + 1}{(\Gamma - 1 + 2\bar{b}\rho_0 + 2Z_0)} \rho_0, \tag{5}$$

$$g = \frac{2(1-\bar{b}\rho_0 - Z_0)}{\Gamma + 1} s, \tag{6}$$

$$p = \frac{2(1-\bar{b}\rho_0 - Z_0)}{\Gamma + 1} \rho_0 s^2 \tag{7}$$

In the present technique of solving the shock wave problem, the undisturbed density ρ_0 varies in accordance with the power law of the radius of the shock front R after the explosion, given as

$$\rho_0 = \rho_a R^\alpha \tag{8}$$

Here, ρ_a and α are regarded as constants. We will determine α later.

IV. PRECISE SOLUTION FOR CONTRACTED MODEL

The R-H conditions (5) – (7) yields the following expression for the pressure behind the shock front

$$p = \frac{(\Gamma - 1 + 2\bar{b}\rho_0 + 2Z_0)}{2(1 - \bar{b}\rho_0 - Z_0)} \rho \mathcal{G}^2 \tag{9}$$

By means of equation (8), equations (2) and (3), can be express as

$$\frac{\partial \mathcal{G}}{\partial t} + \mathcal{G} \frac{\partial \mathcal{G}}{\partial x} + \kappa_1 \left(\frac{\mathcal{G}^2}{\rho} \frac{\partial \rho}{\partial x} + 2\mathcal{G} \frac{\partial \mathcal{G}}{\partial x} \right) = 0 \tag{10}$$

$$\frac{\partial \mathcal{G}}{\partial t} + \mathcal{G} \frac{\partial \mathcal{G}}{\partial x} + \kappa_2 \left(\frac{\partial \mathcal{G}}{\partial x} + \frac{m}{x} \mathcal{G} \right) \mathcal{G} = 0 \tag{11}$$

Where κ_1 and κ_2 are constants given as

$$\kappa_1 = \frac{(\Gamma - 1 + 2\bar{b}\rho_0 + 2Z_0)}{2(1 - \bar{b}\rho_0 - Z_0)},$$

$$\kappa_2 = \frac{(\Gamma - 1 + 2\bar{b}\rho_0 + 2Z_0) [(\Gamma - 1)(\Gamma - 1 + 2\bar{b}\rho_0 + 2Z_0) + \alpha_1(\Gamma + 1)\rho_0] - 2\alpha_2(\Gamma + 1)^2 \rho_0^2}{2 [(\Gamma - 1 + 2\bar{b}\rho_0 + 2Z_0) \{ (\Gamma - 1 + 2\bar{b}\rho_0 + 2Z_0) - \alpha_1(\Gamma + 1)\rho_0 \} + \alpha_2(\Gamma + 1)^2 \rho_0^2]}.$$

By using equation (10) and equation (11) and integrating the result we have got

$$f(t) = \rho \mathcal{G}^\xi x^{-m\eta} \tag{12}$$

The functions $f(t)$ are only functions of time, and ξ and η are constants given as

$$\xi = (2\kappa_1 - \kappa_2) / \kappa_2,$$

$$\eta = \kappa_2 / \kappa_1.$$

By equation (12) and (1), we have

$$\frac{\xi}{\mathcal{G}} \frac{\partial \mathcal{G}}{\partial t} - (1 - \xi) \frac{\partial \mathcal{G}}{\partial x} - \frac{m(\eta + 1)}{x} \mathcal{G} - \frac{1}{f} \frac{df}{dt} = 0 \tag{13}$$

Solving equations (11) and (13), we have

$$\mathcal{G} = -\chi \frac{x}{f} \frac{df}{dt} \quad (14)$$

In which χ is a constant as follows

$$\chi = \frac{1}{(\xi\kappa_2 + \eta + 1)m + (1 + \kappa_2\xi)}. \quad (15)$$

Also,

$$f(t) = f_0 t^{-\tau} \quad (16)$$

here, f_0 represents an arbitrary constant, while constant τ is provided as

$$\tau = \frac{\xi}{\{(\xi - 1)\chi - m(\eta + 1)\chi + 1\}}.$$

Utilizing the R-H condition (6), we can deduce the analytical expression for the shock front radius in the following manner:

$$R(t) = t^{\frac{\Gamma+1}{2(1-\bar{b}\rho_0-Z_0)}\chi\tau} \quad (17)$$

Under the R-H condition (5), α has the value given as

$$\alpha = \frac{2(n+1)(1-\bar{b}\rho_0-Z_0)}{(\Gamma+1)\tau}.$$

Hence, the solution to the problem of a strong shock wave is provided as follows

$$\rho = \frac{f_0 t^{-\tau+\xi} x^{m\eta-\xi}}{\chi^\xi \tau^\xi}, \quad \mathcal{G} = \chi\tau x/t, \quad p = \frac{(\Gamma-1+2\bar{b}\rho_0+2Z_0)}{2(1-\bar{b}\rho_0-Z_0)} \frac{1}{(\chi\tau)^{\xi-2}} f_0 x^{(m\eta-\xi+2)} t^{(\xi-\tau-2)}. \quad (18)$$

In a non-ideal dusty gas, at any given moment, we can compute the total energy (the combined kinetic and thermal energy) within the blast wave by evaluating the density, velocity, and pressure parameters behind the shock front as follows:

$$E = 4\pi \int_0^R \left\{ \frac{1}{2} \rho \mathcal{G}^2 + \frac{(1-Z)(1-\bar{b}\rho)}{\Gamma-1} p \right\} x^m dx, \quad (19)$$

$$\begin{aligned}
 E = At & \frac{(\Gamma+1)\chi\tau\{m(\eta+1)-\xi+3\}}{2(1-\bar{b}\rho_0-Z_0)} + \xi - \tau - 2 + Bt \frac{(\Gamma+1)\chi\tau\{m(\eta+1)-\xi+3\}}{2(1-\bar{b}\rho_0-Z_0)} + \xi - \tau - 2 + Ct \frac{(\Gamma+1)\chi\tau\{m(2\eta+1)-2\xi+3\}}{2(1-\bar{b}\rho_0-Z_0)} + 2\xi - 2\tau - 2 \\
 Dt & \frac{(\Gamma+1)\chi\tau\{m(2\eta+1)-2\xi+3\}}{2(1-\bar{b}\rho_0-Z_0)} + 2\xi - 2\tau - 2 + \\
 Et & \frac{(\Gamma+1)\chi\tau\{m(3\eta+1)-3\xi+3\}}{2(1-\bar{b}\rho_0-Z_0)} + 3\xi - 3\tau - 2,
 \end{aligned} \tag{20}$$

Where, $A = \frac{f_0}{2(\chi\tau)^{\xi-2}\{m(\eta+1)-\xi+3\}}$,

$$B = \frac{f_0(\Gamma-1+2\bar{b}\rho_0+2Z_0)}{2(\Gamma-1)(1-\bar{b}\rho_0-Z_0)(\chi\tau)^{\xi-2}\{m(\eta+1)-\xi+3\}},$$

$$C = \frac{-bf_0^2(\Gamma-1+2\bar{b}\rho_0+2Z_0)}{2(\Gamma-1)(1-\bar{b}\rho_0-Z_0)(\chi\tau)^{2\xi-2}\{m(2\eta+1)-2\xi+3\}},$$

$$D = \frac{-\theta f_0^2(\Gamma-1+2\bar{b}\rho_0+2Z_0)}{2(\Gamma-1)(1-\bar{b}\rho_0-Z_0)(\chi\tau)^{2\xi-2}\{m(2\eta+1)-2\xi+3\}},$$

$$E = \frac{b\theta f_0^3(\Gamma-1+2\bar{b}\rho_0+2Z_0)}{2(\Gamma-1)(1-\bar{b}\rho_0-Z_0)(\chi\tau)^{3\xi-2}\{m(3\eta+1)-3\xi+3\}}.$$

V. RESULTS AND DISCUSSION

The effects of dust particles and non-idealness parameters on the radius of blast wave are shown in figs. 1- 5.

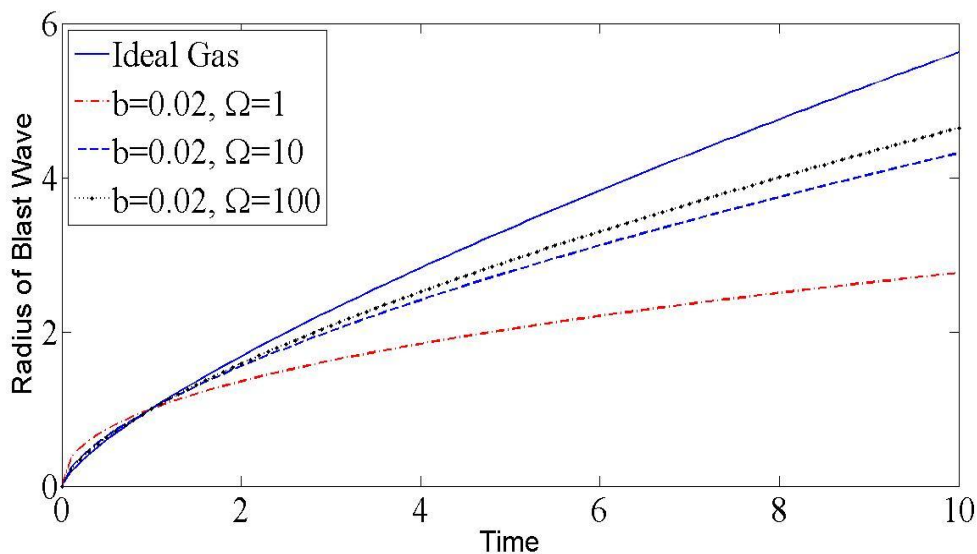


Figure 1: Behavior of the radius of the Blast Wave for $m = 2$.

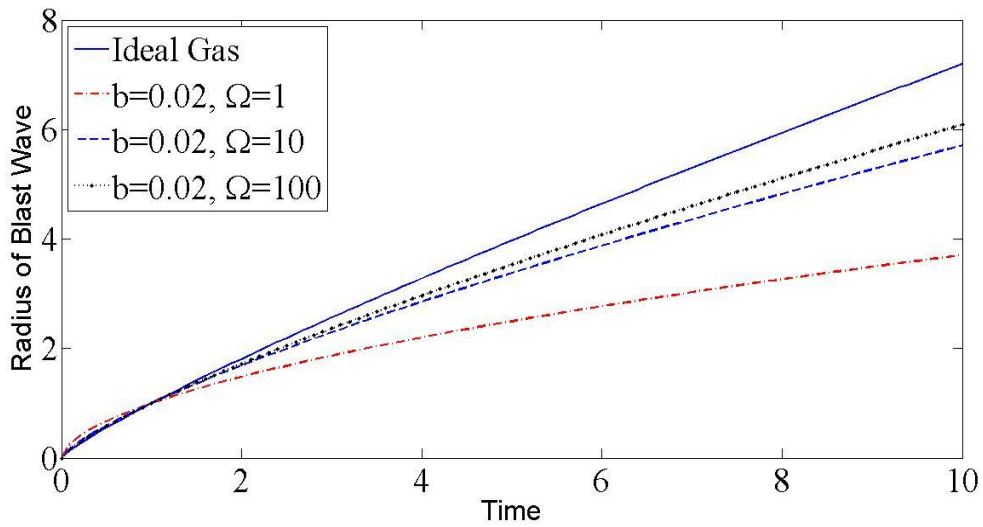


Figure 2: Behavior of the radius of the Blast Wave for $m = 1$.

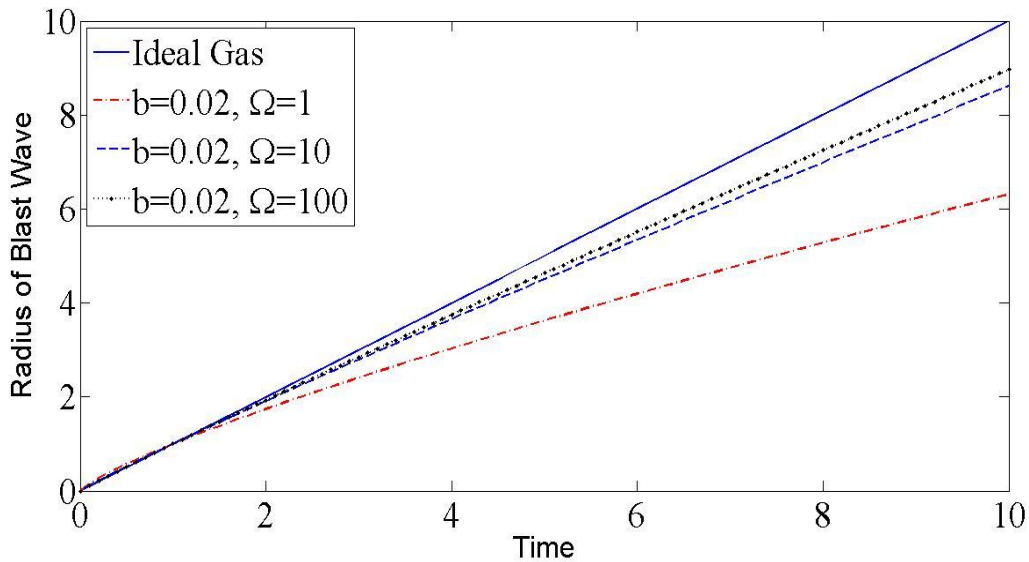


Figure 3: Behavior of the radius of the Blast Wave for $m = 0$.

Figures 1 to 3 show how dust particle density affects blast wave diameter when flowing through planar, cylindrically symmetric and spherically symmetric flows. In the computations, the constants appear as follows:

$$\beta = 0.5 \text{ and } K_p = 0.1, \text{ and } \Omega = 1, 10, 100.$$

It is observed that the radius of blast waves increases with an increase in dust particle density whereas the radius of blast waves decreases with an increase in non-idealness parameter. Based on the data presented in Figure 2 and Figure 3, it is evident that the way the radius of blast wave varies in planar and cylindrically symmetric flows follows a trend that is quite similar to that observed in case of spherically symmetric flow. However, it is important to note that in the planar flow scenario, the rate of this radius variation is notably

slower when compared to both cylindrically symmetric and spherically symmetric flows. Additionally, when we specifically compare the rate of radius variation between cylindrically symmetric and spherically symmetric flows, it becomes apparent that the rate of variation in the cylindrically symmetric flow is also reduced in comparison to the spherically symmetric flow.

The impact of mass fraction and specific heat of dust particles within the mixture on the radius of the blast wave under the conditions of $\Omega = 100$, $\beta = 0.5$ and $\Omega = 100$, $K_p = 1.0$ in spherically symmetric flows are presented in Figures 4 and 5, respectively. It is noteworthy that an increase in the mass fraction of solid particles has a relatively minor effect on the volume fraction of solid particles. However, it exerts a substantial influence on the parameter denoted as Γ . Consequently, an increment in both the mass and specific heat of solid particles leads to a notable enlargement of the blast wave radius.

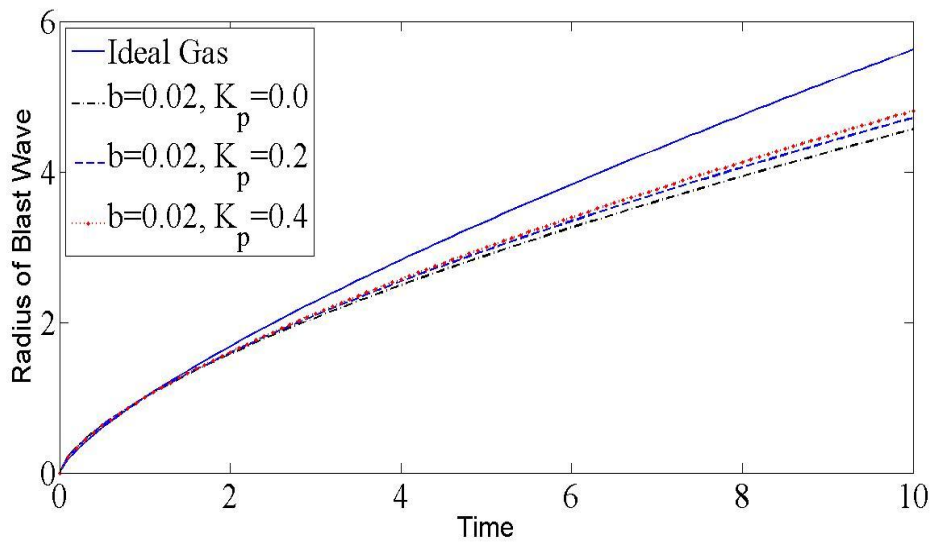


Figure 4: Behavior of the radius of the Blast Wave for $m = 2$.

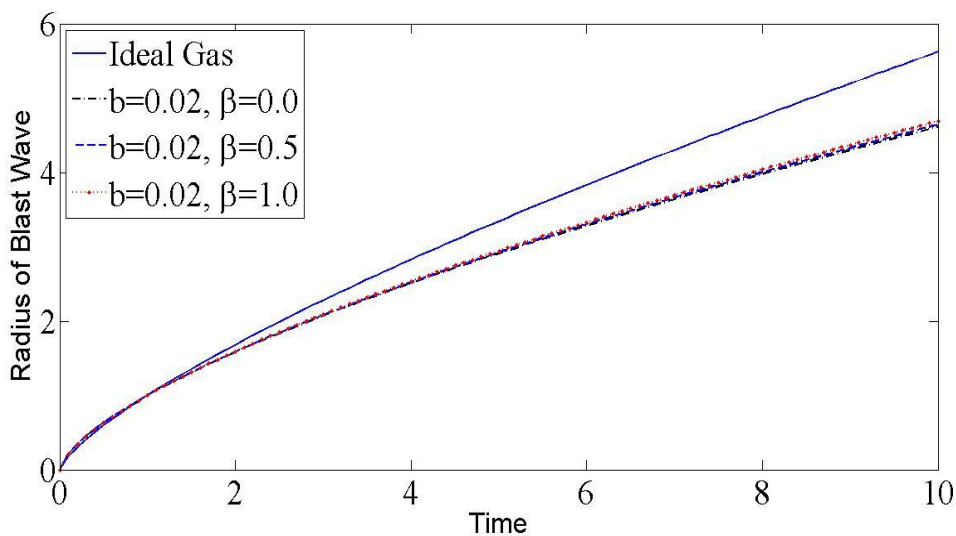


Figure 5: Behavior of the radius of the Blast Wave for $m = 2$.

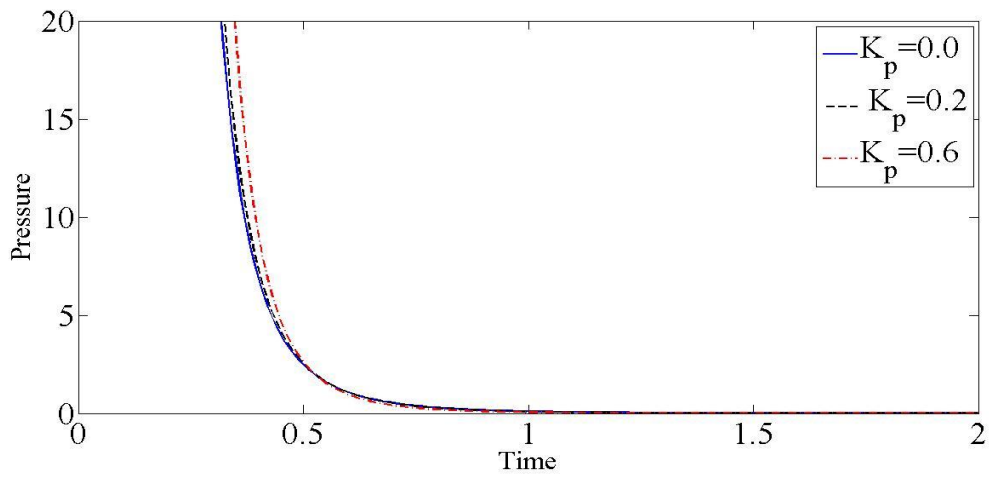


Figure 6: Pressure profile for varying k_p with $b = 0.02$, $\beta = 0.5$ and $\Omega = 100$.

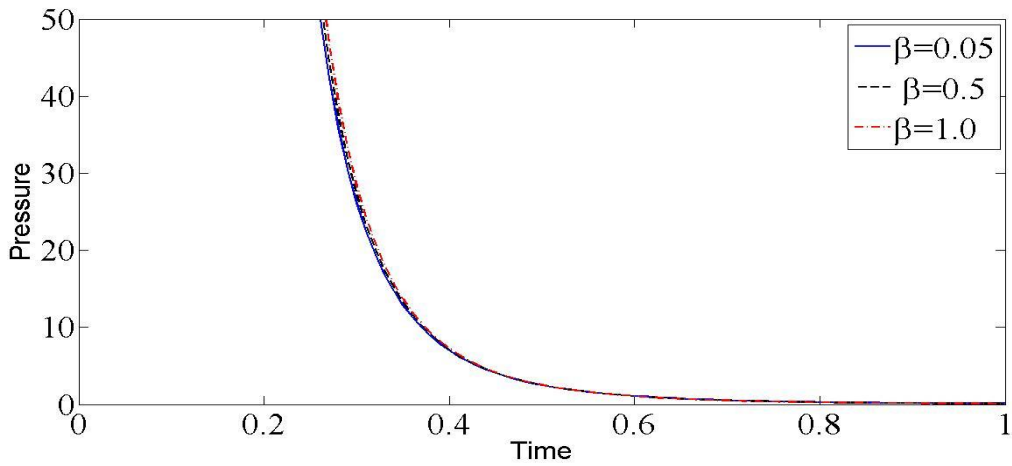


Figure 7: Pressure profile for varying β with $b = 0.02$, $k_p = 0.5$ and $\Omega = 100$.

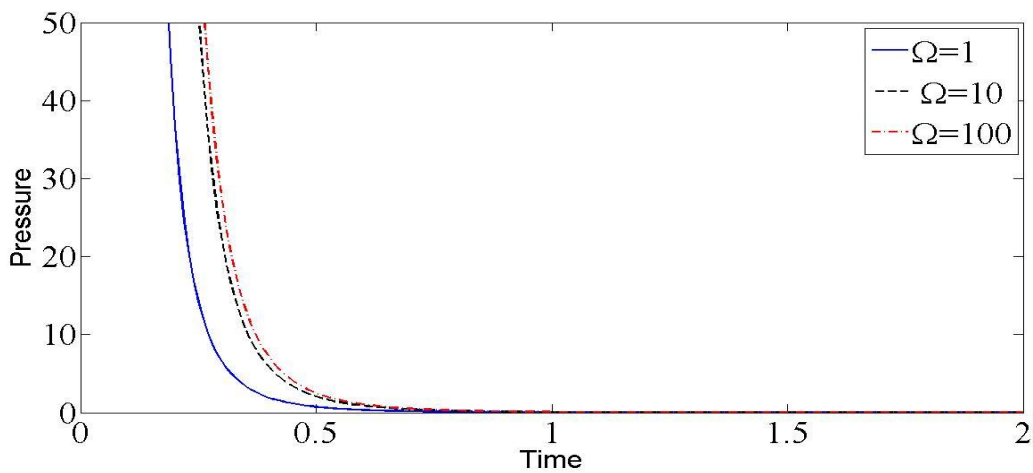


Figure 8: Pressure profile for varying Ω with $b = 0.02$, $\beta = 0.5$ and $k_p = 0.1$.

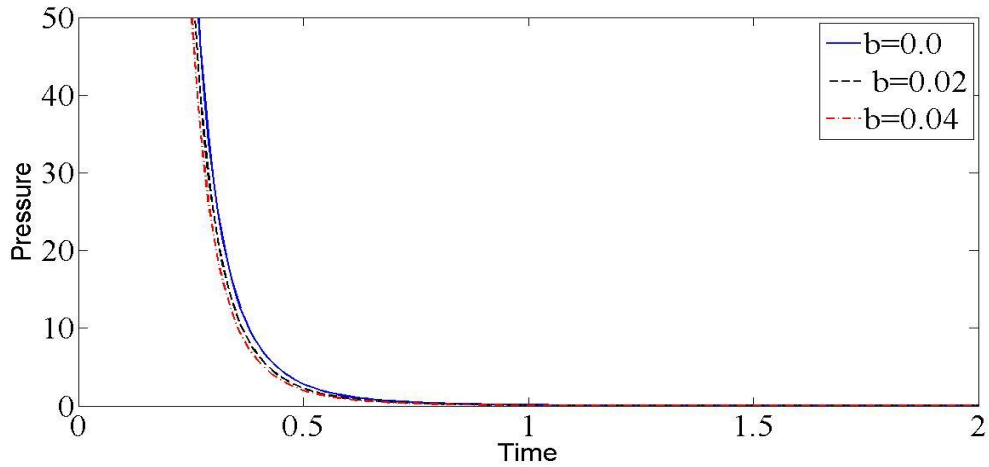


Figure 9: Pressure profile for varying b with $k_p = 0.1$, $\beta = 0.5$ and $\Omega = 100$.

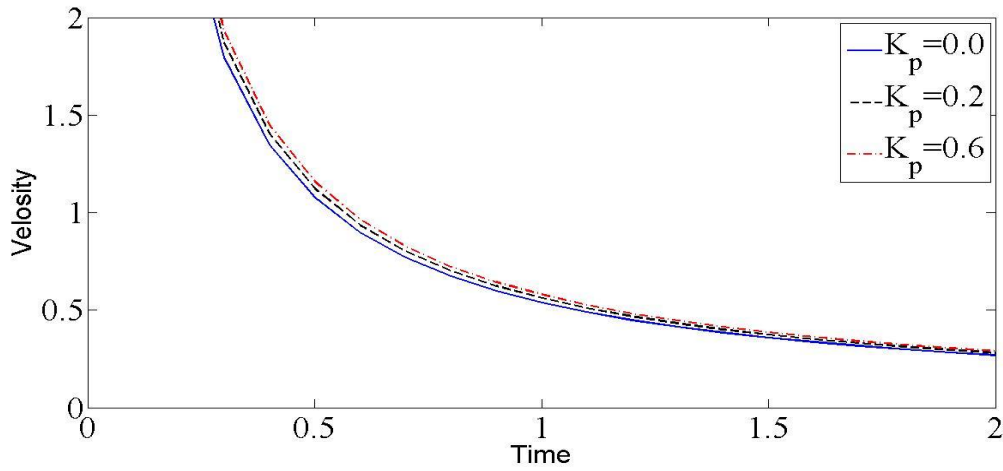


Figure 10: Velocity profile for varying k_p with $b = 0.02$, $\beta = 0.5$ and $\Omega = 100$.

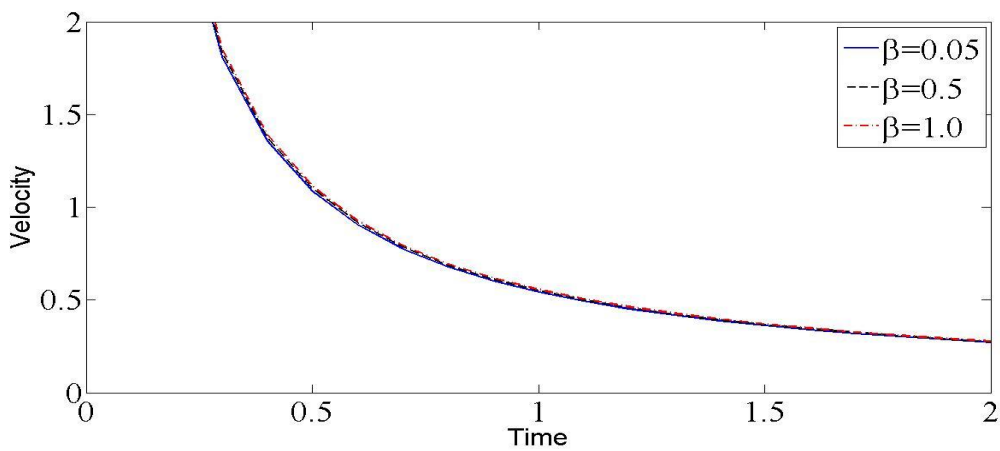


Figure 11: Velocity profile for varying β with $b = 0.02$, $k_p = 0.1$ and $\Omega = 100$.

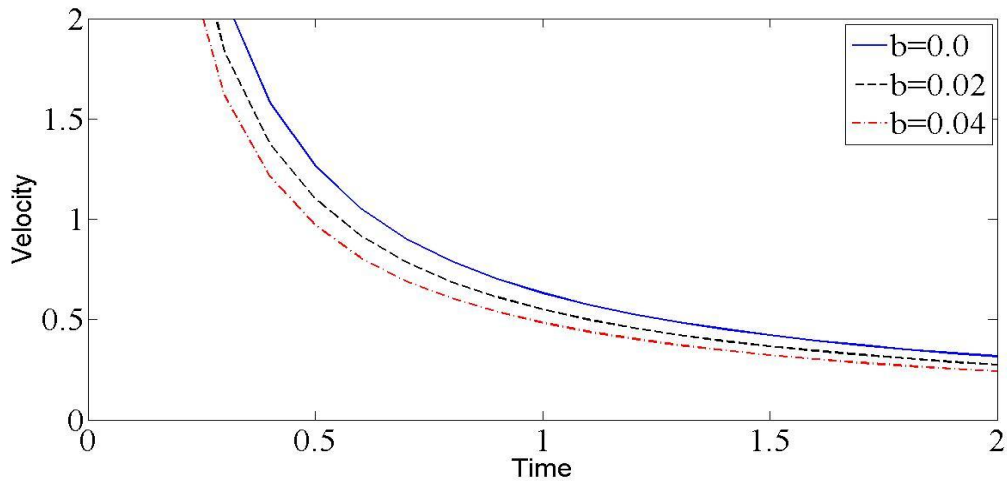


Figure 12: Velocity profile for varying b with $k_p = 0.1, \beta = 0.5$ and $\Omega = 100$.

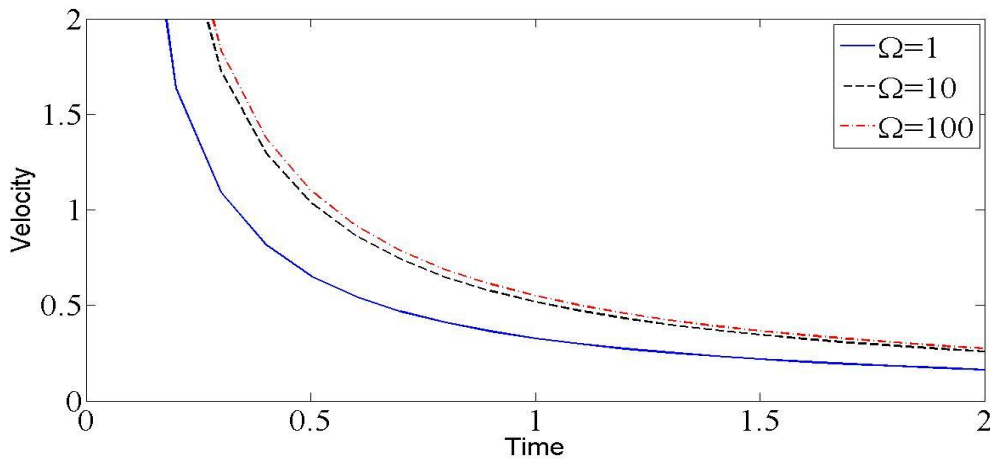


Figure 13: Velocity profile for varying Ω with $b = 0.02, \beta = 0.5$ and $k_p = 0.1$.

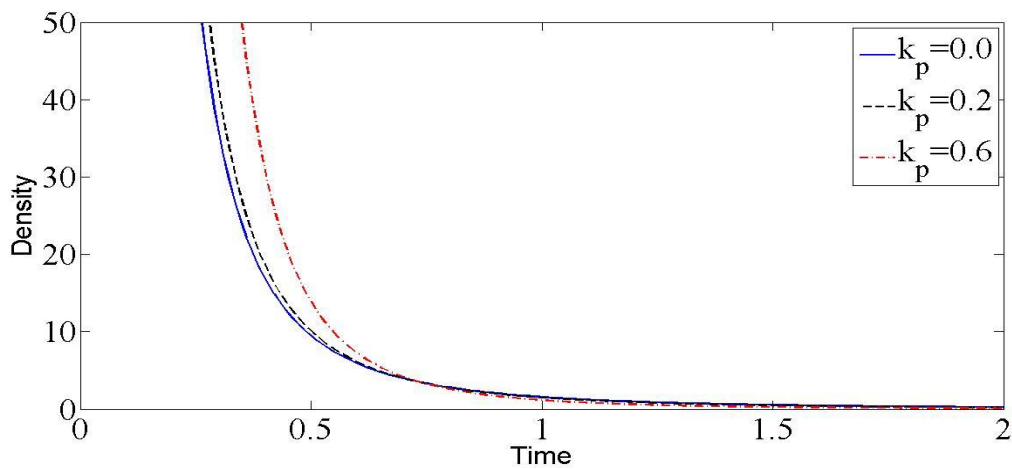


Figure 14: Density profile for varying k_p with $b = 0.02, \beta = 0.5$ and $\Omega = 100$.

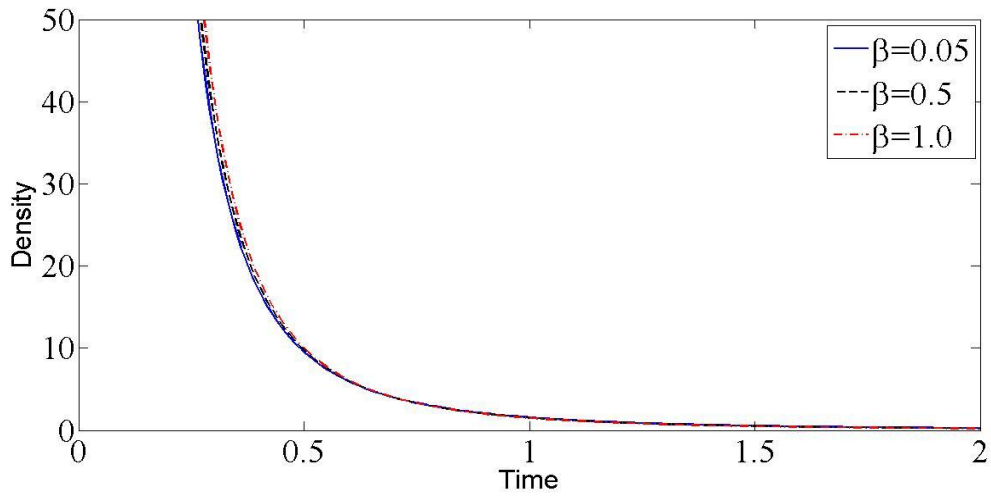


Figure 15: Density profile for varying β with $b = 0.02, k_p = 0.5$ and $\Omega = 100$.

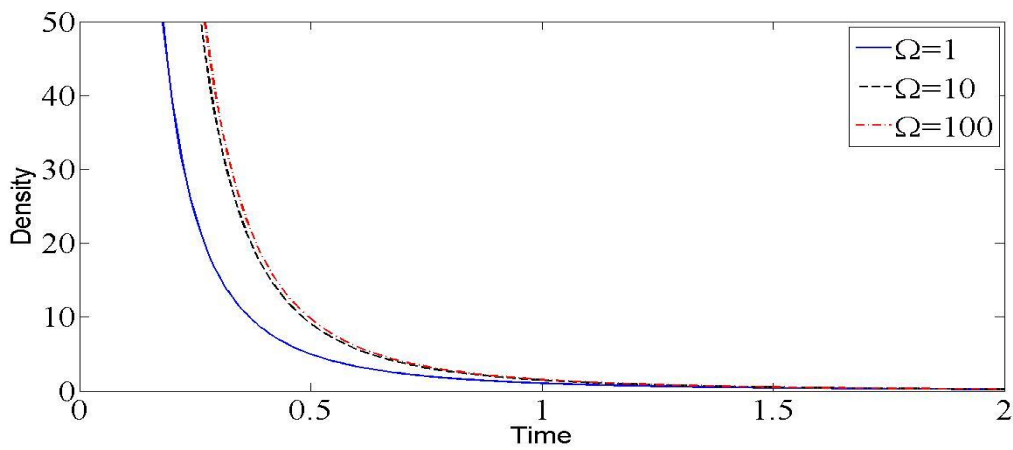


Figure 16: Density profile for varying Ω with $b = 0.02, \beta = 0.5$ and $k_p = 0.1$.

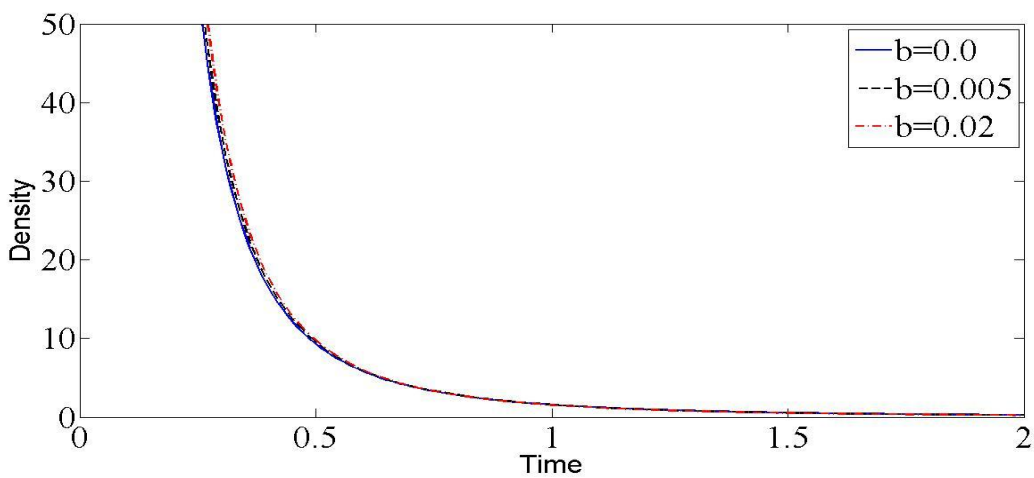


Figure 17: Density profile for varying b with $k_p = 0.1, \beta = 0.5$ and $\Omega = 100$.

The influence of various factors, including dust particles and non-ideal parameters, on spherically symmetric flow fields is depicted in Figures 6 through 17. Upon closer examination, it becomes evident that an increase in any of the following parameters: mass concentration of dust particles, specific heat of solid particles, or species density of solid particles, leads to a corresponding increase in the pressure, velocity, and density of the non-ideal dusty gas. In contrast, the impact of an increase in the van der Waals excluded volume is noteworthy, as it results in a reduction in the pressure, velocity and density of the non-ideal dusty gas.

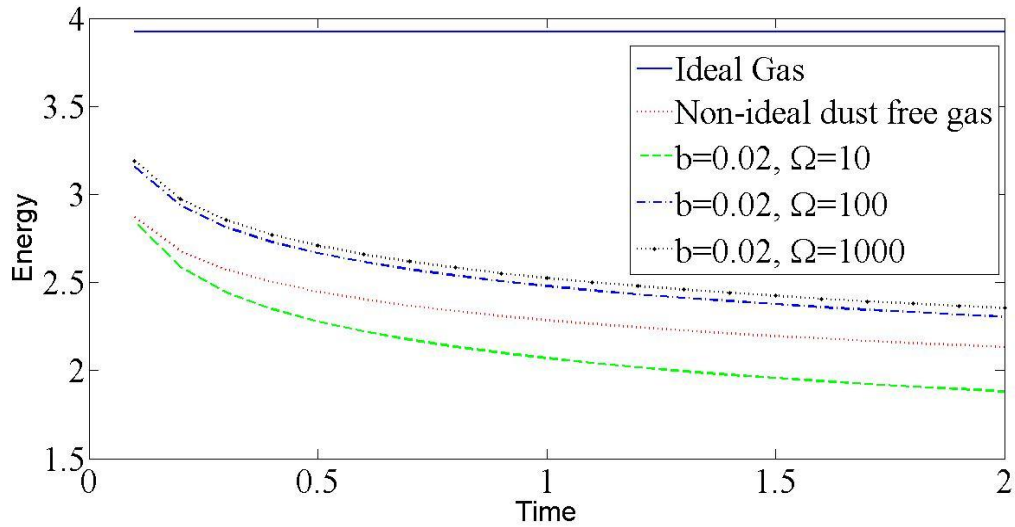


Figure 18: Behavior of energy carried by the blast wave for $m = 2$.

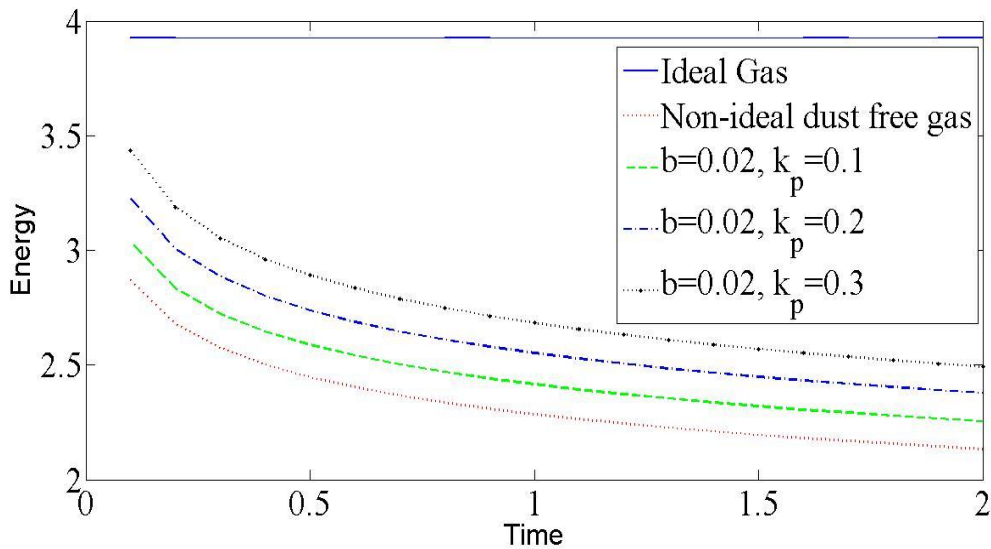


Figure 19: Behavior of energy carried by the blast wave for $m = 2$.

Figure 18 illustrates the impact of two key factors on the energy carried by a blast wave in spherically symmetric flows, the volume fraction of dust particles in the mixture and the non-idealness parameter of the gas. The computations utilize specific constant values, which are provided as follows:

$\beta = 1.0, M_f = 0.1, b = 0.02$ and Volume fraction $\Omega = 0.0, 0.01, 0.02, 0.03, 0.04$ and $\rho_0 = 0, 1, 2, 3, 4$.

In this context, we observe that an increase in the volume fraction of dust particles in the mixture and the non-idealness parameter of gas leads to a reduction in the energy of blast wave within a non-ideal dusty gas.

Figure 19 illustrates how the mass fraction of dust particles in the gas affects the energy of blast wave in spherically symmetric flows. The specific constant values used in the calculations are as follows:

$\beta = 1.0, \Omega = 0.01, b = 0.02$ and mass fraction $M_f = 0.1, 0.2, 0.3, 0.3, 0.4$.

It is noted that the increase in energy carried by the blast wave with a higher dust particle mass fraction can be attributed to several factors. First, the presence of solid particles introduces additional mass to the gas mixture, which, when subjected to the sudden compression and expansion associated with a blast wave, can contribute to an increase in the over all kinetic energy of the system. Since dust particles have a similar impact on the energy carried by a blast wave in both planar and cylindrically symmetrical flows, specific details are omitted.

VI. CONCLUSION

According to our analysis, the solution of the blast wave problem for an adiabatic non-ideal dusty gas given by equation (18) corresponds to that proposed by Murata [6] and Singh *et al.* [15] for $\theta = b = 0$ and to that proposed by Singh *et al.* [7,16], if $\theta = 0, b \neq 0$. This paper presents a new solution to the blast wave problem for non-ideal dusty gas. We also notice that the total energy given by equation (20) is not constant as in Murata [6].

REFERENCES

- [1] G. I. Taylor, Proc. Roy. Soc. A 201, 175 (1950b).
- [2] G. I. Taylor, Proc. Roy. Soc. A 201, 159 (1950a).
- [3] L. I. Sedov, Similarity and Dimensional Methods in Mechanics 1959.
- [4] M. H. Rogers, Astrophys J. 125, 478 (1957).
- [5] P. L. Sachdev, K. T. Joseph and M. Haque Enjnul, Studies in Applied Mathematics 114, 325 (2005).
- [6] S. Murata, Chaos, Solitons and Fractals 28, 327 (2006).
- [7] L.P. Singh, S. D. Ram and D.B. Singh, Chinese Physics Letters, Vol. 28, pp. 114303(1)-114303(3), (2011)
- [8] S.I. Pai, Two Phase Flows, Vieweg Verlag, Braunschweig, 1977 p. 116-167.
- [9] H. Miura and I. I. Glass, Proc. R. Soc. Lond. A 385, 85 (1983).
- [10] M. Chadha and J. Jena, Int. J. Non-Linear Mech. 65, 164 (2014).
- [11] J.S. Díaz and S. E. Rigby, Shock Waves, 32, 405–415 (2022).
- [12] B. Bira and T. Raja Sekhar, Indian J. Pure Appl. Math. 44, 153 (2013).
- [13] V. D. Sharma and R. Shyam, Acta Astronautica 8, 31 (1981).
- [14] H. Sharma and R. Arora, Differ. Equ. Dyn. Syst. 27, 169-180 (2019).
- [15] D. Singh, E. Jain, and S. D. Ram, Indian J Phys (2023). <https://doi.org/10.1007/s12648-023-02864-z>.
- [16] L.P. Singh, S. D. Ram and D.B. Singh, Chaos, Solitons & Fractals, 44, 964-967, (2011)